Molecular Crystals and Liquid Crystals

Experimental study on solid electrolyte interphase of graphite electrode in Li-ion battery by surface analysis technique

Eun Young Jung, Choon-Sang Park, Jae Cheol Lee, Egor Pazhetnov, Kwang Jong Suh, Sung Heo, Tae Eun Hong, Dong Ho Lee, Sung-Il Chien & Heung-Sik Tae

Published online: 04 Jun 2018.

Submit your article to this journal ⬚

View related articles ⬚

View Crossmark data ⬚

Taylor & Francis
Taylor & Francis Group

Check for updates

Experimental study on solid electrolyte interphase of graphite electrode in Li-ion battery by surface analysis technique

Eun Young Jung[a,†], Choon-Sang Park[a,†], Jae Cheol Lee[b], Egor Pazhetnov[c], Kwang Jong Suh[c], Sung Heo[b], Tae Eun Hong[d], Dong Ho Lee[a], Sung-Il Chien[a], and Heung-Sik Tae[a]

[a]School of Electronics Engineering, College of IT Engineering, Kyungpook National University, Daegu, South Korea; [b]Analytical Engineering Group, Samsung Advanced Institute of Technology, Suwon, South Korea; [c]Analysis Group, Samsung SDI Company Ltd., Suwon, South Korea; [d]Division of High-Technology Materials Research, Korea Basic Science Institute, Busan, South Korea

ABSTRACT

This article investigates the characterization of the solid electrolyte interphase (SEI) on the graphite electrode after long cycling times. The chemical composition, molecular structure, and thickness of SEI layer on graphite electrode are characterized by using scanning electron microscope (SEM), X-ray photoelectron spectroscopy (XPS), auger electron spectroscopy (AES), and time of flight-secondary ion mass spectrometry (ToF-SIMS) with respect to cycling times. In particular, we focus the changes in the properties of SEI layer on the graphite electrode surface between initial-state (after 1 cycle) and aged-state (after 500 cycles). More detailed properties of SEI layer after long cycling times are systematically studied by XPS, AES, and ToF-SIMS.

1. Introduction

Commercial lithium-ion cells, with $LiCoO_2$ as the positive electrode, graphite as the negative electrode, and a $LiPF_6$-EC:PC:DEC as electrolyte, were cycled under several conditions of mobile display, portable electronic devices, power tools, and electrical vehicles. During the initial intercalation of lithium ion into the graphite electrode during cycling process, the intercalated lithium reacts immediately with the electrolyte, and forming a passive layer called solid electrolyte interphase (SEI) [1–3]. Therefore, understanding the changes in the chemical composition of the solid electrolyte interphase (SEI) on the electrolyte interface during or after cycling process is important for Li-ion battery (LIB) because the characterization of the SEI significantly affects the performances of LIB, such as cycling life and safety. As the sizes of LIB are becoming larger and their cell sizes are increasing considerably, the importance of life time on the electrolyte is more emphasized. The initial and aged-state of SEI properties has an influence on cell performance such as power capability, low/high temperature performance, and safety. Therefore, it is very important to verify the SEI film formation variations during cycling process in LIB industry. In order to explain the correlation between

SEI property and cell performance, the properties of initial SEI layer on graphite electrode have been reported by means of the scanning electron microscope (SEM), transmission electron microscopy (TEM), Fourier transform infrared spectroscopy (FT-IR), and X-ray photoelectron spectroscopy (XPS) [4–11]. However, the formation variations of SEI layer before and after long-term cycling times are not clearly understood and still controversial over life time. For clarifying the degradation mechanism of battery electrodes due to long-term cycling times, it is necessary to investigate the property of SEI layer on the graphite electrode with respect to cycling times.

In this study, it is necessary to select a stable $LiCoO_2$ which does not change structurally according to long cycle driving. It has been already reported that $LiCoO_2$ is a prevailing material for LIBs because of long lifetime and high energy density compared to other material [12, 13]. Thus, we systematically characterized the chemical composition, molecular structure, and thickness of SEI layer on graphite electrode under various cycling times in real commercial LIB cells (not in coin cell) with $LiCoO_2$ using SEM, XPS, auger electron spectroscopy (AES) and time of flight-secondary ion mass spectrometry (ToF-SIMS) analyses.

2. Experiment

The LIB cells were formed with $LiCoO_2$ active material as the positive electrode and graphite coated with pitch as the negative electrode material, respectively. The negative electrode consists of carbon black for conductivity enhancement and styrene butadiene rubber (SBR) as the binder dissolved in anhydrous N-methyl-2-pyrrolidinone (NMP). The combined carbon black and SBR was coated on a copper foil and was then dried in an oven at 120°C for 1 h. The positive electrode also includes carbon black with $LiCoO_2$ and PVDF binder on an aluminum foil. The thickness for the $LiCoO_2$ and graphite electrode was about 60 μm and 80 μm, respectively. This experiment was used a commercial LIB device of cylindrical type of 18650-model and LIB cells were assembled in a dry room with polyethylene separators between $LiCoO_2$ and graphite electrode. As shown in Table 1, electrolyte was used to 1 M $LiPF_6$ dissolved in the mixtures of ethyl methyl carbonate (EMC), ethylene carbonate (EC), and diethyl carbonate (DEC) in the LIB cells. As additives to the electrolyte solution, vinylene carbonate (VC) and fluoroethylene carbonate (FEC) were used. For the driving of charge and discharge of SEI, the LIB cell was charged to 4.2 V and then discharged to 3.0 V by a constant current-constant voltage (CC-CV) mode for the aging process, and battery electrodes were removed from the cells in an argon-filled glove box after the charge-discharge performance, washed with dimethyl carbonate (DMC) and then transfer vessel to avoid exposure to the air. The morphological property of SEI surface was measured by SEM (Magellan 400, FEI) during various cycling times, using low accelerating voltage of 1 kV. The chemical state of SEI layer was obtained using XPS (ESCA 250, VG Science Inc.), with monochromatized Al Kα radiation (hυ = 1486.6 eV) and an analysis area with a diameter of 500 μm. Charge compensation for the sample was not applied during measurements to avoid damage to the surface structure,

Table 1. Material types of each layers in Li ion battery (LIB) device.

Positive electrode		$LiCoO_2$
Negative electrode		Graphite
Electrolyte	Salt	$LiPF_6$
	Solvent	DMC: EC: EMC
	Additives	FEC

and the pressure in the analysis chamber was kept below 1.0×10^{-9} Torr. For high resolution measurements of the elements, constant pass energy was set to 24.5 eV. The spectrometer was calibrated using the photoemission line Ag $3d_{5/2}$ (binding energy 368.3 eV). For the Ag $3d_{5/2}$ line the full width at half maximum (FWHM) was 0.58 eV. The binding energy of all acquired spectra was corrected to the C1s peak at 285 eV [8, 9]. The relative thickness of SEI layer was estimated by AES (PHI 710, ULVAC-PHI) on the graphite electrode for initial-state (after 1 cycle) and aged-state (after 500 cycles). The AES depth profile was conducted under conditions of 3 keV, 6 µA Ar^+ ion beam in a 1 mm × 4 mm area for depth profiling of SEI. The sputtering rate has been verified with calibration on SiO_2/Si wafer (SiO_2 thickness 40nm basing on ellipsometry data). Sputtering rate was estimated as much as 41 nm/min under conditions of 3 keV, 6 µA Ar^+ ion. In order to obtain the chemical composition of SEI layer, Tof-SIMS measurement was performed using a spectrometer (IonTOF 5, ION-TOF) with a 25 keV, Bi_3^+ primary ion beam. The current and an analysis area were 0.5 pA and 500 µm × 500 µm, respectively. Secondary ions were observed in the positive and negative ion mode, and a full spectrum from 1 amu to 2000 amu was detected.

3. Results and discussion

Figure 1 shows the SEM images of the SEI layer on graphite electrode after cycling performance with respect to different cycling times. As shown in Fig. 1, the reaction compounds derived from the decomposition products of electrolyte were observed to be increased on the SEI layer as the cycling times increased.
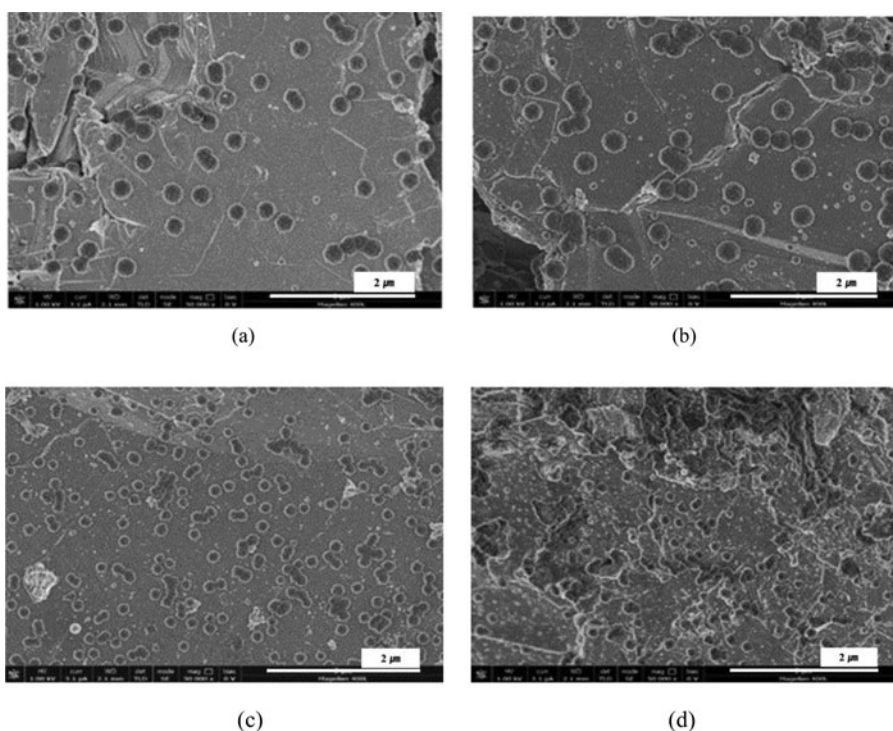

(a)

(b)

(c)

(d)

Figure 1. Scanning electron microscopy (SEM) images with respect to cycling times. (a) initial-state (after 1 cycle), (b) after 100 cycles, (c) after 300 cycles, and (d) after 500 cycles.
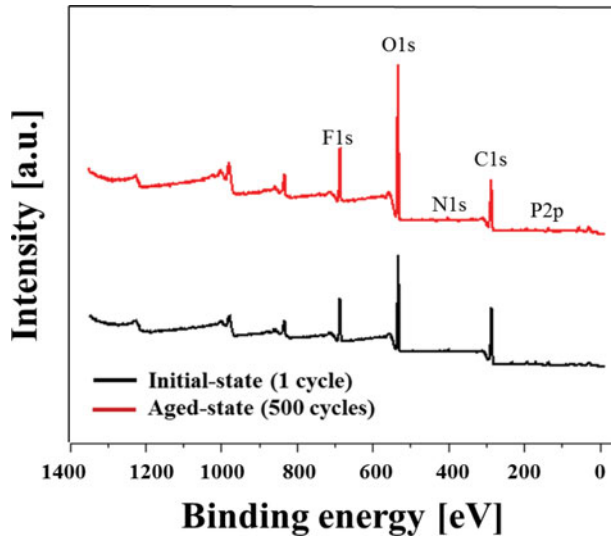
Figure 2. X-ray photoelectron spectroscopy (XPS) survey spectra of solid electrolyte interphase (SEI) on the graphite electrode surface with respect to degradation conditions (or cycling times) such as (a) initial-state (after 1 cycle) and (b) aged-state (after 500 cycles).

Figure 2 shows the XPS survey spectra of SEI on the graphite electrode surface with respect to the degradation conditions such as the initial-state (after 1 cycle) and aged-state (after 500 cycles). The XPS atomic concentrations of survey spectra on the graphite electrode are summarized in Table 2. There was a clear difference between the initial-state and aged-state. The atomic concentrations of oxygen (O1s) and lithium (Li1s) on the surface region of the electrode for aged-state case were larger than those of electrode with the initial-state. On the other hand, the atomic concentrations of fluorine (F1s) and phosphate (P2p) at surface region of the electrode for aged-state case were less than those of initial-state.

To analyze the chemical bonding states of the SEI surface on the graphite electrode for initial and degradation after 500 cycles, XPS narrow-scan spectra (C1s, F1s, P2p, O1s, and Li1s) of SEI layer were obtained in Fig. 3. As shown in Table 3, the F1s spectra were fitted with two peaks centered at 687.5 eV (reduction products of $LiPF_6$) and 685.5 eV (lithium fluoride, Li-F), respectively. The P2p spectra were fitted with two peaks centered at 134 eV (P-O bond)

Table 2. X-ray photoelectron spectroscopy (XPS) compositions (at%) of graphite electrode surfaces for initial-state (after 1 cycle) and aged-state (after 500 cycles).

Atomic%	C1s	O1s	F1s	P2p	N1s	S2p	Li1s
Initial-state (1 cycle)	43.3	22.7	9.8	2.2	1.1	1.3	19.6
Aged-state (500 cycles)	32.5	26.7	8.5	1.6	0.7	0.5	29.5

Table 3. Different surface species estimated from peak area of F1s and P2p using XPS high resolution narrow scan spectra for initial-state (after 1 cycle) and aged-state (after 500 cycles).

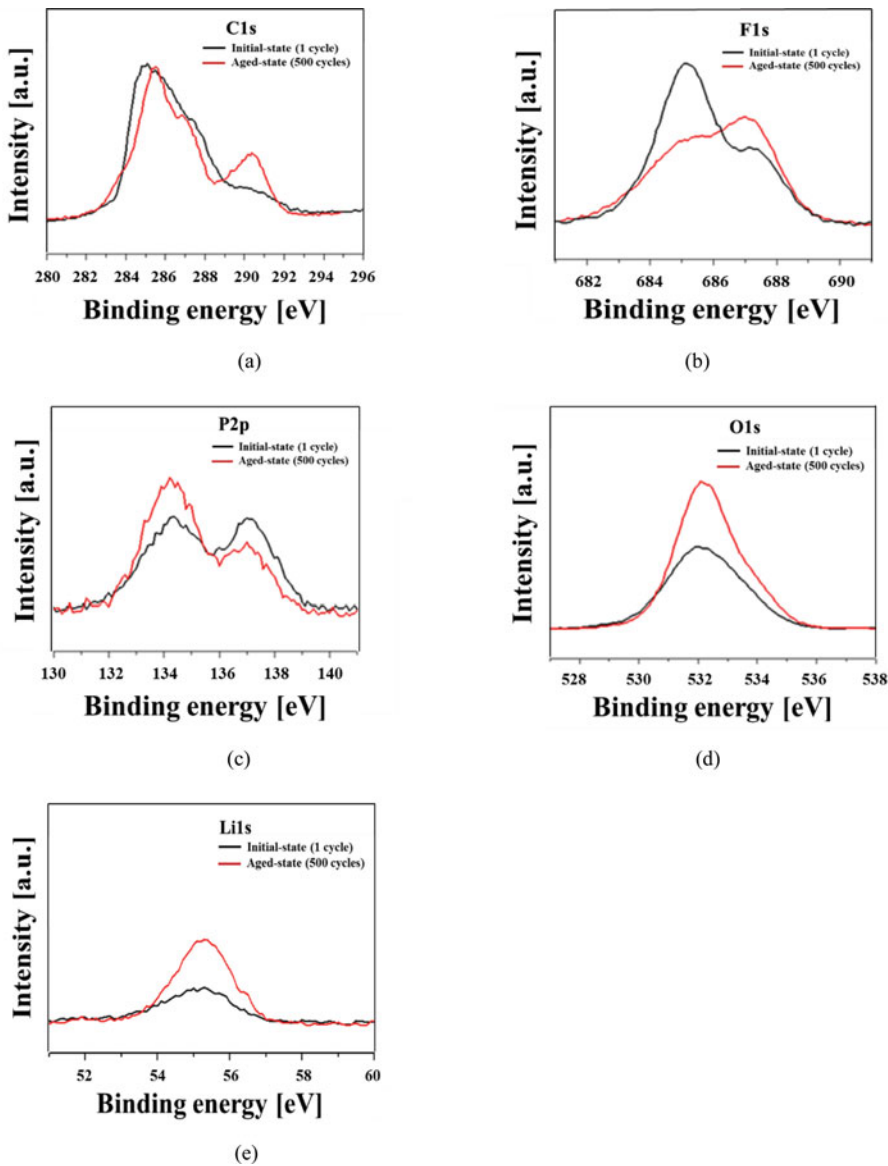|	F1s (%)		P2p (%)	
	685 eV Li-F	688 eV P-F,C	134–135 eV P-O	137–138 eV P-F
Initial-state (1 cycle)	74.6	25.4	55.4	44.6
Aged-state (500 cycles)	48.2	51.8	70.8	29.2

Figure 3. XPS narrow scan high resolution spectra of SEI on the graphite electrode with respect to degradation conditions such as (a) initial-state (after 1 cycle) and (b) aged-state (after 500 cycles).

and 138 eV (P-F bond) [8, 9]. The XPS results show that the SEI layer of the initial-state had higher concentrations of carbon and fluorine than those of aged-state. After 500 cycles, the surface of SEI was observed to contain a low concentration of lithium fluoride and high concentration of oxygen, which meant that the reaction compounds from the electrolyte consisting of Li and O were increased on the electrode during charge-discharge cycling performance, thereby resulting in decreasing the carbon and fluorine after long-term cycling process. As shown in Fig. 3(c) and Table 3, in the case of aged-state, the P-O bond (134 eV) of XPS chemical state in SEI layer was increased due to the increase in the oxygen elements, whereas, after 500 cycles, the P-F bond (138 eV) of chemical state in SEI on the graphite electrode was decreased.
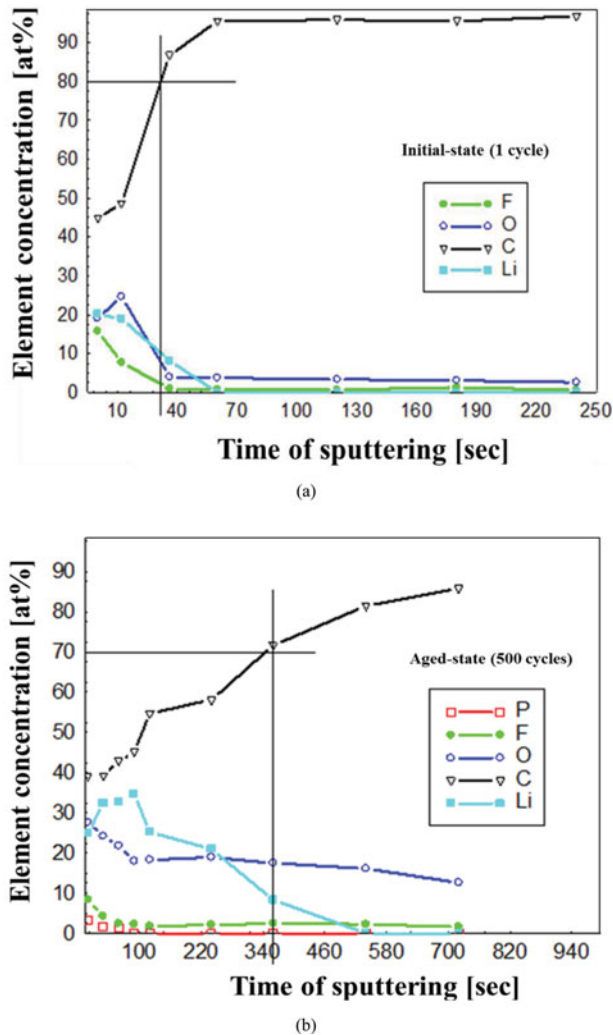
Figure 4. Auger electron spectroscopy (AES) depth profiles of SEI on the graphite electrode surface with respect to degradation conditions such as (a) initial-state (after 1 cycle) and (b) aged-state (after 500 cycles).

In order to obtain the relative thickness of SEI layer on the graphite particle, we measured the AES depth profile mode. Figure 4 shows the AES depth profiles of SEI layer on the graphite surface for the initial-state (after 1 cycle) and aged-state (after 500 cycles). The sputtering rate for the instrument has been verified with calibration on SiO_2/Si wafer (SiO_2 thickness 40 nm basing on ellipsometry data). The etching rate with an argon gun can roughly determine the thickness using a SiO_2 sample (41 nm/min) as a reference. Although this measured SEI thickness might not indicate the absolute value, this procedure could lead to understanding appropriately and to comparing relatively the SEI thicknesses. Based on this measurement, the calculated thicknesses for the initial-state and aged-state were 20 nm and 200 nm, respectively. The AES results show that the thickness of the aged-state was thicker than that of initial-state, as shown in Fig. 4. The reason for the thickness increase with aging was originated in the deposited reaction compounds, and derived from the decomposition products of electrolyte, on SEI layer after 500 cycles.
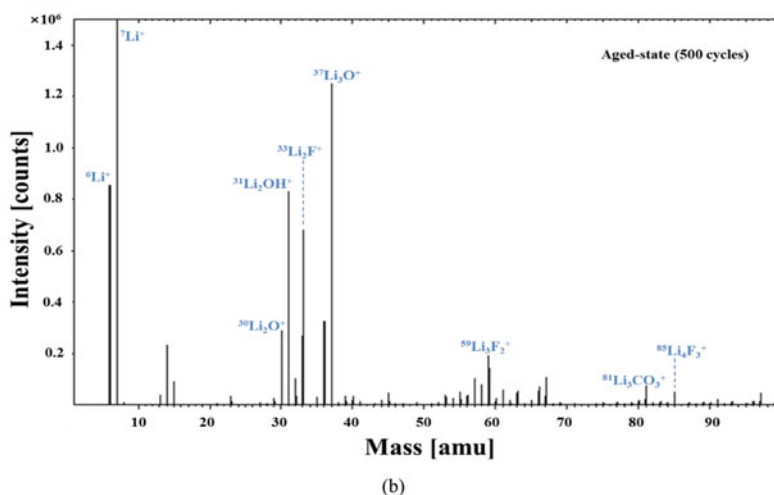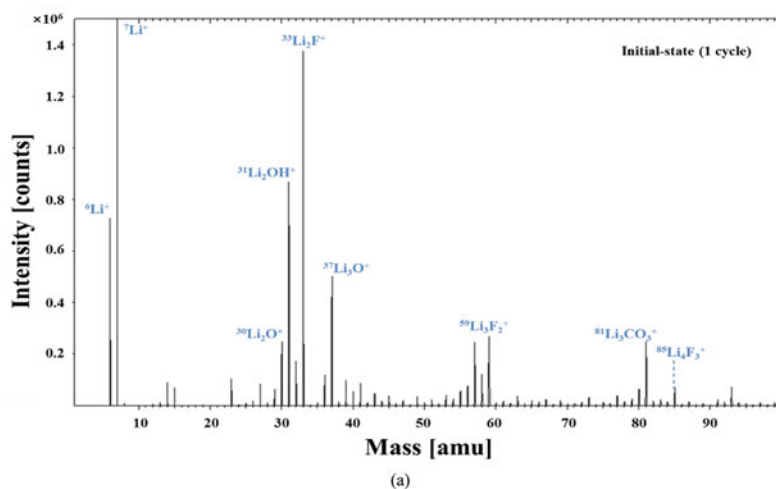
Figure 5. Positive ion spectra using time of flight-secondary ion mass spectrometry (ToF-SIMS) of SEI on the graphite electrode surface for (a) initial-state (after 1 cycle) and (b) aged-state (after 500 cycles).

In order to determine the specific chemical structures for SEI layer on the graphite electrode surface, we measured the positive and negative ion mode using ToF-SIMS method. Figure 5 shows the ToF-SIMS positive ion mass spectra of SEI on the graphite electrode surface for the initial-state (after 1 cycle) and aged-state (after 500 cycles). The ToF-SIMS results represent that $Li_{n+1}F_n^+$ (n = 1–3) peaks, derived from lithium fluoride, were observed at both cases. These lithium fluorides are originated from the preferential reaction of FEC electrolyte. In the case of aged-state, the surface of graphite electrode had a smaller $Li_{n+1}F_n^+$ peaks than those of initial-state. This result is in good agreement with the XPS results. Additionally, some peaks detected such as $^{31}Li_2OH^+$, $^{37}Li_3O^+$, and $^{81}Li_3CO_3^+$ were due to the decomposed compounds of EC and DEC electrolyte in LIB [10, 11]. After 500 cycles, the electrode surface had a higher $^{37}Li_3O^+$ peak than that of initial-state.

Figure 6 shows the ToF-SIMS negative ion mass spectra of SEI on the graphite electrode surface for the initial-state (after 1 cycle) and aged-state (after 500 cycles). As shown in Fig. 6, negative ion mass spectra of ToF-SIMS show the major two peaks, such as $^{19}F^-$ and $^{145}PF_6^-$, which is originated from $LiPF_6$ electrolyte. After 500 cycles, the graphite electrode had smaller
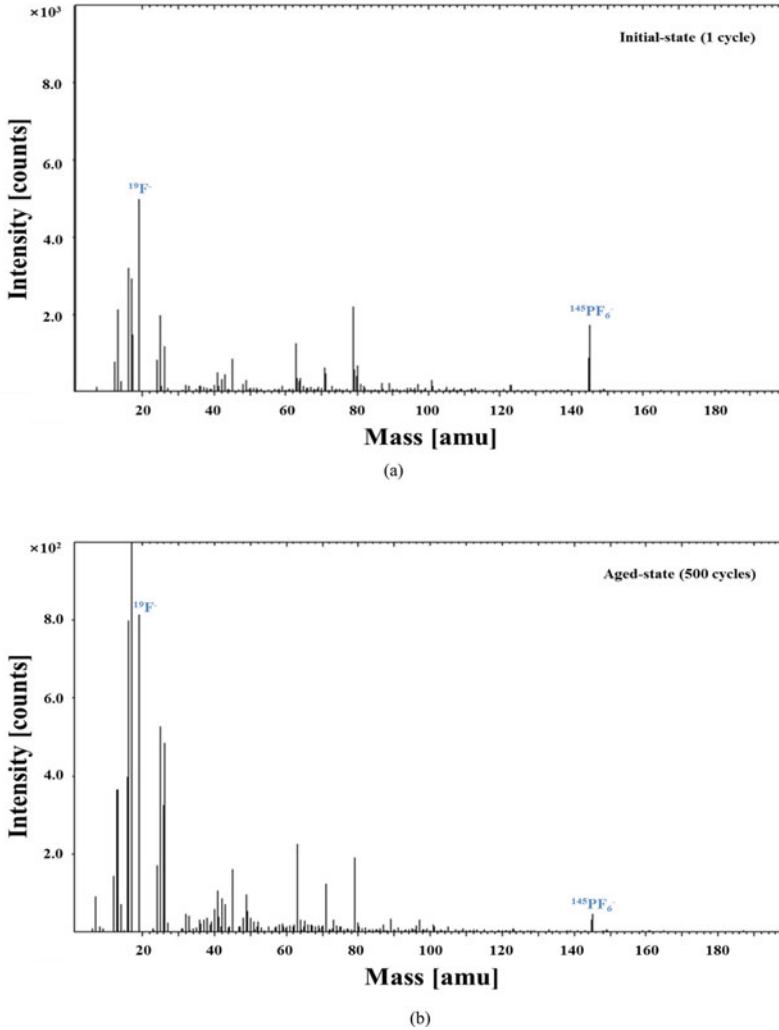
Figure 6. Negative ion spectra using ToF-SIMS of SEI layer on the graphite electrode for (a) initial-state (after 1 cycle) and (b) aged-state (after 500 cycles).

Table 4. Peaks identifications observed in positive-ion spectra using time of flight-secondary ion mass spectrometry (ToF-SIMS) of solid electrolyte interphase (SEI) layer on the graphite electrode.

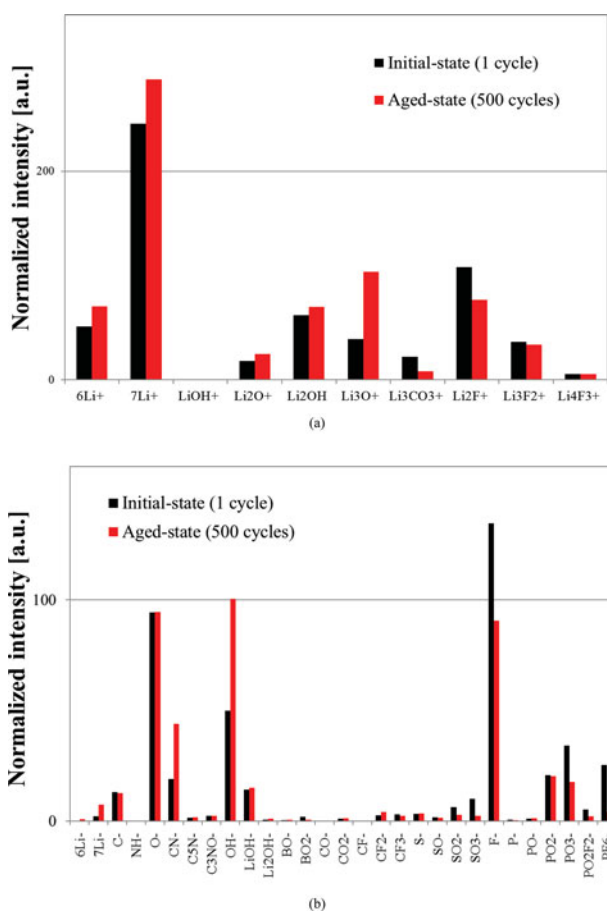| Positive ion mass spectrum m/z	Possible ion fragment/possible structure
6, 7	Li^+
31	Li_2OH^+
33	Li_2F^+
37	Li_3O^+
59	$Li_3F_2^+$
81	$Li_3CO_3^+$
85	$Li_4F_3^+$

Figure 7. Normalized intensity ratio of (a) positive and (b) negative ions obtained on the graphite electrode surface using ToF-SIMS for (a) initial-state (after 1 cycle) and (b) aged-state (after 500 cycles).

^{19}F$^-$ and ^{145}PF$_6^-$ peaks than those of initial-state. Also, the graphite electrode for the aged-state case had larger OH$^-$ peaks than those of initial-state. These results are in good agreement with the XPS results.

    Figure 7 represents the normalized intensities of the positive and negative ions obtained on the surface of graphite electrode surface for the initial-state (after 1 cycle) and aged-state (after 500 cycles). Peaks identifications observed in the positive and negative ion ToF-SIMS spectra of SEI layer on the graphite electrode surface are listed in Tables 4 and 5, respectively. As shown

Table 5. Peaks identifications observed in negative-ion spectra using ToF-SIMS of SEI layer on the graphite electrode.

Negative ion mass spectrum *m/z*	Possible ion fragment/possible structure
7	Li$^-$
19	F$^-$
31	P$^-$
47	PO$^-$
63	PO$_2^-$
79	PO$_3^-$
145	PF$_6^-$

in Fig. 7, the ToF-SIMS results show that the SEI layer for the aged-state case contained a low concentration of lithium fluoride and high concentration of oxygen compounds, respectively. These results may postulate that the top layer of the SEI surface for the aged-state case mainly consisted of the lithium compound, such as $^{31}Li_2OH^+$, $^{37}Li_3O^+$, and $^{81}Li_3CO_3^+$, after the long-term cycling times.

4. Conclusions

In this study, various surface analyses techniques such as XPS, AES and ToF-SIMS are examined in order to measure the detailed characteristics of SEI layer on the graphite electrode before and after the degradation. The XPS result shows that the fluorine and carbon elements on the SEI for the aged-state after 500 cycles are decreased, whereas the oxygen element is increased, compared to those of the initial-state after 1 cycle. This result means that the reaction compounds produced from the electrolyte comprising of Li and O are increased on the electrode during the charge-discharge cycling performance, thereby reducing the carbon and fluorine after long-term cycling process. The ToF-SIMS result reveals that the SEI layer for the aged-state case contained a low concentration of lithium fluoride ($Li_{n+1}F_n^+$) and high concentration of oxygen compounds such as $^{81}Li_3CO_3^+$, $^{33}Li_3O^+$ and $^{31}Li_2OH^+$, derived from the decomposition of electrolytes. Additionally, the thickness of SEI layer on the graphite particle is measured by AES depth profile mode, and is observed to be increased after 500 cycles. The reason for this increase in the thickness of SEI layer as a result of long-term cycling process would be presumably due to both the deposited reaction compounds and the decomposition products of electrolyte on the SEI layer after 500 cycles. Based on these measurement results of the XPS, ToF-SIMS, and AES, the guidelines can be provided for measuring the detail information of SEI layer in order to understand the degradation mechanism after long-term cycling time in LIB.

Funding

References

[1] Birkl, C. R., Roberts, M. R., E., M., & Bruce, P. G. (2017). *J. Power Sources*, *341*, 373.
[2] Waldmann, T. et al. (2016). *J. Electrochem. Soc.*, *163*(10), A2149.
[3] Schronder, K. et al. (2015). *Chem. Mater.*, *27*, 5531.
[4] Abe, K. et al. (2004). *J. Electrochem. Acta.*, *49*(26), 4613.
[5] Abe, K. et al. (2004). *Electrochem. Solid-State Lett.*, *7*, 462.
[6] Zhang, Q. et al. (2005). *Chem. Lett.*, *34*, 1012.
[7] Lee, J. T. et al. (2013). *CARBON*, *52*, 388.
[8] Lee, S. H. et al. (2014). *J. Power Sources*, *247*, 307.
[9] Lee, S. H., Jo, I. S., & Kim. (2014). *Surf. Interface Anal.*, *46*, 570.
[10] Nakai, H., Kubota, T., Kita, A., & Kawashima, A. (2011). *J. Electrochem. Soc.*, *158*(7), A798.
[11] Kubota, T., Ihara, M., Katayama, S., Nakai, H., & Ichikawa, J. (2012). *J. Power Sources*, *207*, 141.
[12] Tebbe, J. L., Fuerst, T. F., & Musgrave, C. B. (2016). *ACS Appl. Mater. Interfaces*, *8*(40), 26664.
[13] Song, B. H. et al. (2015). *J. Mater. Chem. A*, *3*, 18171.